CVD synthesis of Cu_2O films for catalytic combustion of VOCs

Guan-Fu Pan, Shi-Bin Fan, Jing Liang, Yue-Xi Liu, Zhen-Yu Tian*

Institute of Engineering Thermophysics, Chinese Academy of Sciences, Beijing, China

Abstract

Catalytically active thin films of Cu_2O were synthesized by a home-made pulsed-spray evaporation chemical vapor deposition for the deep oxidation of C_2H_2 and C_3H_6. The obtained films were comprehensively characterized with X-ray diffraction (XRD), Scanning electron microscopy (SEM) and X-ray photoelectron spectroscopy (XPS). The results indicate that the prepared films at 270 ℃ are pure Cu_2O and none of the impurities could be detected. The catalytic tests reveal that the synthesized Cu_2O leads the complete oxidation decreased by 250 ℃ for C_3H_6 and 175 ℃ for C_2H_2 relative to the non-coated mesh with good reusability and reproducibility.

1. Introduction

Volatile organic compounds (VOCs) are the main air pollutants emitted from the combustion of fossil fuels in many industry processes and transportation activities. VOCs are associated with various health-related problems. Catalytic combustion was commonly used for the abatement of VOCs in the past decades. The involved catalysts are mainly composed of noble metals such as Au, Pt and Rh [1-3] and transition metal oxides (TMOs). Noble metals generally exhibit good catalytic performance, but they are expensive and easy to be poisoning. For these reasons, catalytic oxidation of VOCs over TMOs has captured increasing attention, and considerable efforts have been devoted to the synthesis and application of TMOs for such purposes [4-7]. Specifically, CuO, Co_3O_4, Mn_3O_4 and Fe_2O_3 exhibited good performance as active catalysts for VOCs treatment [8-12].

Compared to other TMOs, Cu_2O owns attractive stability and has excellent catalytic applications for VOCs [13]. Rostami and Jafari used Cu_2O nanoparticles as catalysts to remove aromatic compounds. They reported that Cu_2O was an efficient catalyst at 350 ^oC [6]. Barreca et al. used Cu_2O films on Al_2O_3 subtrates as gas sensor in the detection of VOCs. Kim and Shim investigated the catalytic characteristic of Cu_2O and concluded that Cu_2O was active for the removal of VOCs [13].

Several methods were involved in the production of Cu_2O, such as sol-gel [14], top-down approach with nanosecond and picosecond lasers [15], honey aided solution synthesis [16], electrochemical synthesis [17] and photonic crystal template-assisted electrodeposition [18]. In recent years, pulsed-spray evaporation chemical vapor deposition (PSE-CVD) has been successfully used to prepare a series of TMOs, e.g., Co_3O_4 and Mn_3O_4. Compared to the above-mentioned techniques, PSE-CVD is easy to control the thickness and quality of the films and relatively cheap. Thus, PSE-CVD exhibits potential to prepare Cu_2O thin films.

In the current work, the Cu_2O thin films were synthesized by a home-made PSE-CVD system for the deep oxidation of VOCs with C_2H_2 and C_3H_6 existed in the exhaust emissions as representatives. The prepared Cu_2O samples were characterized in terms of structure, morphology and composition.

2. Material and methods

2.1 Preparation of Cu_2O thin films

The Cu_2O thin films were synthesized in a PSE-CVD system combined with cold-wall stagnation point-flow CVD reactor and waste collector, as presented in Fig. 1. The preparation process consists of four steps.Firstly, copper acetylacetonate ($Cu(acac)_2$) was dissovled in ethanol at a concertration of 2.5 mM, which was delivered as liquid feedstock by a PSE unit. The PSE delivery frequency was set at 4 Hz and the opening time of PSE was 2.5 ms. The feeding rate was 1.03 mL/min. The evaporation chamber is 30 cm long and kept at 3000 Pa and 180 ℃. Secondly, the resulting vapor was transported into the deposition chamber with O_2 and N_2 with flowrates of 1.0 and 0.5 standard liter per minute (SLM), respectively. Thirdly, the Cu_2O thin films were formed on different substrates (planar glass, silicon, stainless steel and mesh grid) kept at 270 ^oC. Finally, the waste vapor was collected by a liquid nitrogen trap.

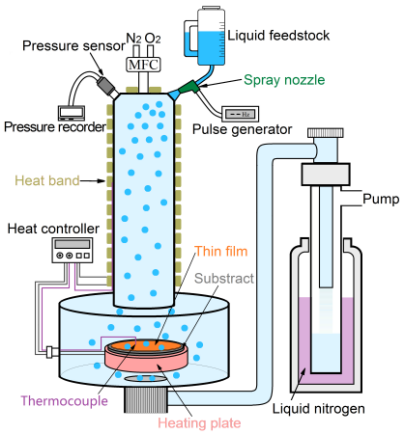

Fig. 1 Schematic diagram of the PSE-CVD system.

2.2 Characterization

The obtained Cu_2O films were characterized in terms of structure, morphology and chemical composition with X-ray diffraction (XRD), Scanning

* Corresponding author: tianzhenyu@iet.cn

electron microscopy (SEM) and X-ray photoelectron spectroscopy (XPS), respectively. XRD analysis was performed on Bruker D8 Focus with Cu Kα radiation, scan angle of 5-90^{o} and scanning step of 0.02^{o}. The microstructure was examined using SEM (S-4800 Hitachi) with the resolution of 1.5 nm (15 KV). The chemical composition was identified by the XPS (ESCALAB 250Xi) with pass energy of 20 eV and energy step size of 0.050 eV. The XPS results were analyzed by Avantage. The elemental content in the film samples was quantitative analyzed by non-linear least square fitting method and the form of oxygen was analyzed by Unimodal fitting method [19].

2.3 Catalytic test

The performances of the Cu_2O films for C_2H_2 and C_3H_6 conversion were investigated by a fixed bed quartz reactor, as shown in Fig. 2. A 60 cm long alundum tube (8.0 mm inner diameter) was fixed in a digital electrical furnace. 20 mg of the Cu_2O supported on grid mesh of stainless steel was put in the same temperature area. A K-thermocouple was used to measure the temperature of Cu_2O film. A gas mixture consisted of 1 % fuel gas (C_2H_2 or C_3H_6), 10 % O_2 and 89 % Ar was introduced into the alundum tube with a total flow rate of 15 ml/min. The temperature of this furnace rised with a ramp of 2 ^{o}C/min from 150 to 1000 ^{o}C. Finally, the exhausting gas was measured by a gas chromatograph (NETZSCH, GC3000) for a quantitative analysis.

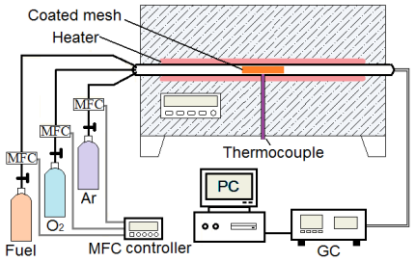

Fig. 2 Experimental setup of catalytic test.

3. Results and discussion

3.1 Growth

By measuring the weight difference of the substrates before and after deposition, the growth of the prepared films can be estimated. Five experiments at different total deposition time were carried out on the mesh grid of stainless steel and the result is displayed in Fig. 3. A linear behavior is observed and the growth rate of Cu_2O is calculated to be 1.6 nm/min. The results indicate that the synthesis of Cu_2O with PSE-CVD system can be tailored with respect to thickness.

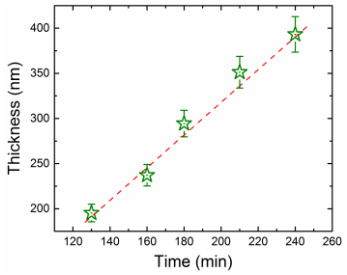

Fig. 3 Growth of Cu_2O thin film.

3.2 Phase identification

The X-ray diffraction pattern of the obtained thin film is shown in Fig. 4. The well-defined diffraction peaks are observed at 29.73 °, 36.41 °, 42.24 °, 61.88 ° and 73.81 °, which can be well attributed to (110), (111), (200), (220) and (311) orientations of Cu_2O in the literature (JCPDS no. 05-0667). No characteristic peaks of any other impurities were observed in the XRD patterns, indicating the formation of monoclinic Cu_2O phase [20,21]. The sharp and strong reflection peaks suggest that the as-prepared samples are well crystallized. The crystallite size and the micro-strain of Cu_2O thin films were calculated to be 29 nm and 0.0583 by applying Scherrer's formula: $D = 0.9\lambda/\beta \cos\theta$; and the equation $\varepsilon = \beta/2\cot\theta$ to the most intense diffraction peak, where $\lambda = 0.154056$ nm and where β and θ represent the full width at half maximum and diffraction angle of the observed peak, respectively [22].

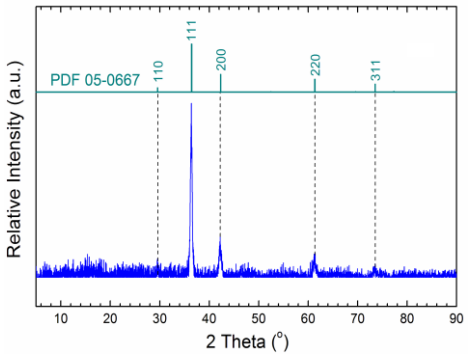

Fig. 4 XRD pattern of the prepared Cu_2O thin film.

3.3 Microstructural studies

SEM inspection was carried out to reveal the morphology of the as-obtained Cu_2O samples. The representative SEM images with different magnifications are shown in Fig. 5. The SEM images reveal that the film is homogeneous and is composed of a large quantity of small ball-like particles. The particle size is estimated to be 30 nm, which agrees well with the crystallite size calculated by XRD results. Besides the ball-like shapes, a number of hollows are also observed. These hollows could adsorb more oxygen than the smooth surface, which would benefit for the catalytic oxidation of VOCs.

3.4 Surface composition

In order to explore the chemical composition of the Cu_2O films, ex situ XPS analysis was performed on both bare and etched surfaces. By comparing the numerical contents of C 1s, O 1s and Cu 2p shown in Table 1, it can be easily found that the content of Cu raises and O decreases as the depth deepens from surface (non-etched) to 95 nm etched. Based on the XPS results, the Cu/O atomic ratio of 95 nm etched layer was estimated to be about 2, which is consistent with the form of Cu2O obtained with XRD analysis.

As indicated in Fig. 6, the components of the as-synthesized thin films are mainly consist of Cu and O from the entire XPS spectrum (Fig. 6a). As exhibited in Fig. 6b, the Cu 2p 1/2 peak is centered at 952.25 eV and

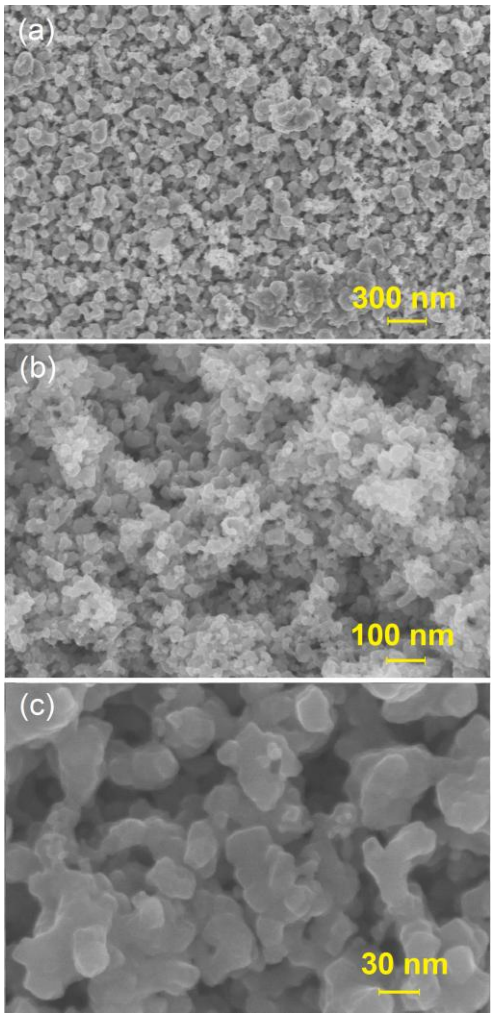

Fig. 5 SEM images of thin Cu_2O films at different magnifications.

the Cu 2p 3/2 peaks at 932.35 eV [23]. It should be noted that the content of C 1s is negligible after 95 nm etching Since Cu 2p can hardly differentiate Cu^{2+} and Cu^{1+}, it is necessary to involve analysis of auger spectrum. The Cu auger spectrum of obtained thin film was shown in Fig. 7a. The obvious peak located at 916.80 eV is perfectly coinciding with the standard Cu_2O auger spectrum. The binding energies of O 1s

Table 1 Chemical composition of Cu_2O thin films

Non – etched		
	Peak BE	Proportion (%)
C 1s	284.78	17.11
O 1s	529.87	43.73
Cu 2p	933.62	39.16
5.7 nm – etched		
	Peak BE	Proportion (%)
C 1s	284.80	6.12
O 1s	529.61	41.99
Cu 2p	932.35	51.89
95 nm – etched		
	Peak BE	Proportion (%)
C 1s	284.78	1.54
O 1s	530.14	35.62
Cu 2p	932.37	62.84

were observed to be 529.65 and 531.45 eV (see Fig. 7b), corresponding to the lattice oxygen (O_L) and adsorbed oxygen (O_{ads}), respectively. The fitted profiles agree well with the measured profiles, as shown in Fig. 7.

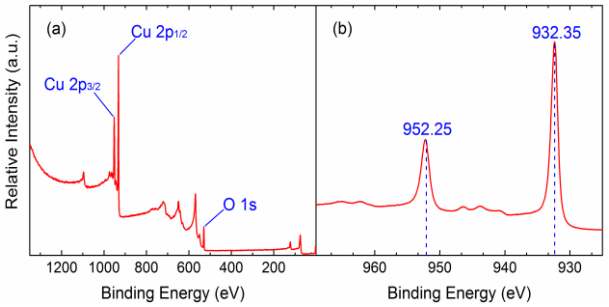

Fig. 6 Entire XPS spectrum (a) and Cu 2p spectrum (b).

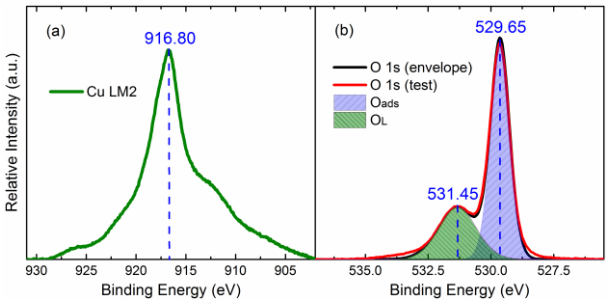

Fig. 7 Cu LM2 (a) and O 1s signals (b) of a representative Cu_2O thin film.

3.5 Catalytic performance

The catalytic performance of the Cu_2O grown on mesh of stainless of steel was tested for the complete oxidation of C_2H_2 and C_3H_6 at atmospheric pressure. The background effect of the stainless steel element on the oxidation was examined by carrying out the experiments on non-coated mesh (NCM) under the same conditions. Figure 8 compares the temperature-dependent conversion ratio of C_2H_2 and C_3H_6 with Cu_2O coated mesh and non-coated mesh. Compared to the non-coated mesh condition, the complete oxidation of C_2H_2 decreased from 450 ^oC to 300 ^oC and for C_3H_6 decreased from 675 ^oC to 425 ^oC with Cu_2O. The catalytic tests were carried out three times for the same sample and the results are quite close, demonstrating that the prepared Cu_2O has good reusability with reprodued results.

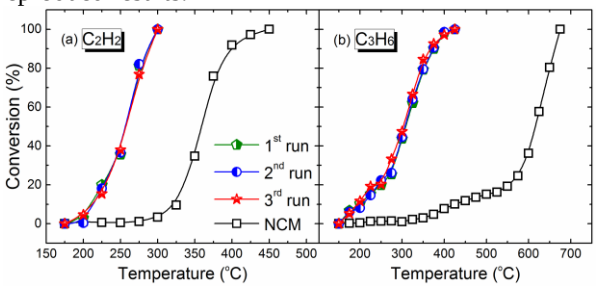

Fig. 8 Conversion profiles of C_2H_2 and C_3H_6 over mesh grid of stainless steel coated with Cu_2O and non-coated mesh (NCM).

Figure 9 presents the releases of CO_2 and CO in the oxidation processes on both Cu_2O-coated mesh and

non-coated mesh. The maximum temperatures of CO_2 release in the oxidation processes of C_2H_2 and C_3H_6 agree well with the complete oxidation of C_2H_2 and C_3H_6. During the oxidation of C_2H_2 and C_3H_6 over Cu_2O-coated mesh, CO was not detected. However, a number of CO was measured over non-coated mesh, which could come from the partial oxidation. Based on the XPS results, both the lattice and adsorbed oxygen in the Cu_2O films could lower down the energy barrier for the complete oxidation and prevent from the formation of CO. Moreover, the hollow ball-like revealled by the microstructure analysis could expose more surface area and adsorbe more oxygen, which would make the oxidation occur at relatively low temperatures.

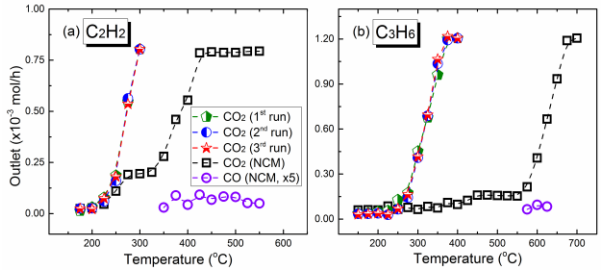

Fig. 9 Outlet profiles of CO and CO_2 during the catalytic tests.

4. Conclusions

This work presents a detailed introduction of facile synthesis of Cu_2O thin films by using a home-made PSE-CVD system for catalytic oxidation of C_2H_2 and C_3H_6. XRD, SEM and XPS were employed to characterize the physicochemical properties of the deposited films with respect to phase, morphology and surface composition. The catalytic performance against deep oxidation of C_2H_2 and C_3H_6 over Cu_2O samples was tested at atmospheric pressure in a fixed-bed quartz reactor. XRD analysis indicates that the prepared films at 270 ℃ are pure Cu_2O and none of the impurities could be detected. The results show that the Cu_2O leads the complete oxidation decreased by 175 ℃ for C_2H_2 and 250 ℃ for C_3H_6 relative to the non-coated mesh. According to the microstructure and XPS results, the lattice and adsorbed oxygen as well as the hollow ball-like geometry could benefit for the deep oxidation of C_2H_2 and C_3H_6. These results reveal that transition metal oxides, especially Cu_2O can be easily prepared and show good potential in the catalytic abatement of VOCs.

Acknowledgements

ZYT thanks the financial support from the Recruitment Program of Global Youth Experts (Grant No. Y41Z024BA1).

References

[1] S. Ivanova, C. Petit, V. Pitchon, Gold Bulletin 39 (2006) 3.
[2] A.C. Gluhoi, N. Bogdanchikova, B.E. Nieuwenhuys, Journal of Catalysis 232 (2005) 96.
[3] T. Maillet, C. Solleau, J. Barbier-Jr, D. Duprez, Applied Catalysis B-Environmental 14 (1997) 85.
[4] M.H. Khedr, K.S.A. Halim, M.I. Nasr, A.M. El-Mansy, Materials Science and Engineering a-Structural Materials Properties Microstructure and Processing 430 (2006) 40.
[5] H.Y. Lin, Y.W. Chen, W.J. Wang, Journal of Nanoparticle Research 7 (2005) 249.
[6] R. Rostami, A.J. Jafari, Journal of Environmental Health Science and Engineering 12 (2014) 1.
[7] P. Mountapmbeme Kouotou, Z.Y. Tian, H. Vieker, K. Kohse-Höinghaus, Surface and Coatings Technology 230 (2013) 59.
[8] C.Q. Hu, Q.S. Zhu, Z. Jiang, Y.Y. Zhang, Y. Wang, Microporous and Mesoporous Materials 113 (2008) 427.
[9] S. Somekawa, T. Hagiwara, K. Fujii, M. Kojima, T. Shinoda, K. Takanabe, K. Domen, Applied Catalysis A-General 409 (2011) 209.
[10] A. Urbutis, S. Kitrys, Chemija 24 (2013) 111.
[11] Z.Y. Tian, P. Mountapmbeme Kouotou, N. Bahlawane, P.H. Tchoua Ngamou, Journal of Physical Chemistry C 117 (2013) 6218.
[12] S.R. Wang, H.X. Zhang, Y.S. Wang, L.W. Wang, Z. Gong, Rsc Advances 4 (2014) 369.
[13] S.C. Kim, W.G. Shim, Applied Catalysis B-Environmental 79 (2008) 149.
[14] P. Mallick, Proceedings of the Natinal Academy of Sciences India Section A-Physical Sciences 84 (2014) 387.
[15] M. Ali, F. Yehya, A.K. Chaudhary, V.V.S.S. Srikanth, Conference on Light and Its Interactions with Matter 1620 (2014) 327.
[16] M. Ali, N.K. Rotte, V.V.S.S. Srikanth, Materials Letters 128 (2014) 253.
[17] F. Hu, K.C. Chan, T.M. Yue, C. Surya, Thin Solid Films 550 (2014) 17.
[18] J.P. Zhang, L.P. Yu, Journal of Materials Science-Materials in Electronics 25 (2014) 5646.
[19] M.C. Biesinger, L.W.M. Lau, A.R. Gerson, R.S.C. Smart, Applied Surface Science 257 (2010) 887.
[20] J. Medina-Valtierra, J. Ramirez-Ortiz, V.M. Arroyo-Rojas, F. Ruiz, Applied Catalysis A-General 238 (2003) 1.
[21] G.G. Condorelli, G. Malandrino, I. Fragala, Chemistry of Materials 6 (1994) 1861.
[22] Z.Y. Tian, N. Bahlawane, V. Vannier, K. Kohse-Höinghaus, Proceedings of the Combustion Institute 34 (2013) 2261.
[23] X.S. Jiang, M. Zhang, S.W. Shi, G. He, X.P. Song, Z.Q. Sun, Journal of the Electrochemical Society 161 (2014) D640.